arXiv:1405.4609v1 [cond-mat.stat-mech] 19 May 2014

Scaling analysis of stationary probability distributions of random walks on one-dimensional lattices with aperiodic disorder

Hiroshi Miki*

Department of Applied Science for Electronics and Materials,

Interdisciplinary Graduate School of Engineering Sciences,

Kyushu University, 6-1 Kasuga-Koen, Fukuoka 816-8580, Japan

(Dated: May 20, 2014)

Abstract

Stationary probability distributions of one-dimensional random walks on lattices with aperiodic disorder are investigated. The pattern of the distribution is closely related to the diffusional behavior, which depends on the wandering exponent Ω of the background aperiodic sequence: If $\Omega < 0$, the diffusion is normal and the distribution is extended. If $\Omega > 0$, the diffusion is ultraslow and the distribution is localized. If $\Omega = 0$, the diffusion is anomalous and the distribution is singular, which shows its complex and hierarchical structure. Multifractal analysis are performed in order to characterize these distributions. Extended, localized, and singular distributions are clearly distinguished only by the finite-size scaling behavior of $\alpha_{\min}$ and $f(\alpha_{\min})$. The multifractal spectrum of the singular distribution agrees well with that of a simple partitioning process.

PACS numbers: 05.40.Fb, 05.45.Df

* Present address: Research Institute for Humanity and Nature, 457-4 Motoyama Kamigamo, Kita-ku, Kyoto 603-8047, Japan.

I. INTRODUCTION

Random walks have long been one of the most fundamental processes both in physics and mathematics[1]. Due to their simplicity and interesting and rich structure, they provide the basis for understanding many kinds of physical phenomena, including transport processes, fluctuating time series, relaxation processes, and pattern formation. It is well known that for a random walk on a symmetric and homogeneous background, the average displacement vanishes and the average mean-square displacement scales linearly with time:

$$< X(t) >= 0, \tag{1}$$

$$< X^2(t) > \sim t. \tag{2}$$

On the other hand, it is also known that the diffusional behavior of the system is strongly and qualitatively modified by disorder, especially when the spatial dimension is low. In a one-dimensional random walk with random disorder, the diffusion is strongly suppressed and the average mean-square displacement grows on a log-time scale [3, 4]:

$$< X^2(t) > \sim (\log t)^4, \tag{3}$$

which is called ultraslow diffusion.

In this article we consider systems with aperiodic disorder. An aperiodic disorder is generated by a certain deterministic rule. It is this point that distinguishes aperiodic from random disorder. We expect that the behavior of systems with aperiodic disorder is, in general, intermediate between that of homogeneous system and that of system with random disorder. In fact, for a random walk on a certain particular one-dimensional lattice with aperiodic disorder, it was reported in ref.[2] that an anomalous diffusion may occur. This is characterized as

$$< X^2(t) > \sim t^{\phi}, \quad \text{with } 0 < \phi < 1. \tag{4}$$

Interestingly these normal, ultraslow, and anomalous diffusion are observed in dynamical deterministic maps[5]. Recently an unified understanding of the diffusional behavior described by Eqs.(2)-(4) has been attempted from the point of view of a weakly chaotic regime of a deterministic map[6]. In addition to the theoretical and mathematical interest, systems with aperiodic disorder have been fabricated artificially[7].

We investigate the structure of the stationary probability distribution of a random walk on a one-dimensional lattice with aperiodic disorder. For a one-dimensional lattice, aperiodic

disorder is expressed by a corresponding aperiodic sequence. It is the wandering exponent Ω that characterizes an aperiodic disorder and affects the diffusional behavior. It determines how the geometrical fluctuation of the sequence Δ scales with the length of the sequence L, $\Delta \sim L^{\Omega}$[2, 8, 9]: If Ω is negative, the geometrical fluctuation is bounded and the effect of the disorder becomes smaller as the size of the system grows. Therefore, the diffusional behavior becomes qualitatively similar to that on a homogeneous background. On the other hand, if Ω is positive, the effect of the disorder becomes stronger with an increase in the system size. If Ω vanishes, the effect of the disorder is almost independent of the system size - the fluctuation grows logarithmically. In this case we observe anomalous diffusion, which is written as Eq.(4).

Therefore, we expect that the stationary probability distribution will show a characteristic pattern. Furthermore, we expect the pattern to depend on only the wandering exponent and to correspond to the diffusional behavior. We do not expect it to depend on the details of the aperiodic sequence.

Here we consider random walks on one-dimensional lattices, for which the disorder is constructed by the Thue-Morse (TM), the Rudin-Shapiro (RS), and the paperfolding (PF) sequences, which are taken as representative examples. The TM, RS, and PF sequences have negative, positive and vanishing wandering exponents, respectively. They have several properties in common: 1) They are binary sequences, *i.e.*, they are composed of two types of symbols, A and B; 2) They are constructed systematically from the initial sequences and by the substitution rules; 3) The ratio of the number of A to that of B converges to unity in the limit of infinite length. In these cases the geometrical fluctuation of the sequence is given by the difference between the number of A and that of B.

Multifractal analysis will be used to characterize the structure of the stationary probability distribution. Suppose that a probability distribution is given and the support of the distribution is covered with patches of size ϵ. Let $p_j(\epsilon)$ be the measure assigned to the j-th patch. It is expected that the measure scales with ϵ as

$$p_j(\epsilon) \sim \epsilon^{\alpha_j}, \tag{5}$$

where α_j is the singularity exponent. It is also expected that the number of patches which takes the value of the singularity exponent between α and $\alpha + d\alpha$ also scales as

$$N(\alpha)d\alpha \sim \epsilon^{-f(\alpha)}d\alpha, \tag{6}$$

where $f(\alpha)$ is, roughly speaking, the fractal dimension of the set of patches with α. Multifractal analysis has been applied to characterize the scaling structure of various distributions including those of the quantum localization problem[11], energy dissipation in turbulence[12, 13], and the sidebranch structure of dendrites[14]. Since it is so widely applicable, we expect that multifractal analysis will also be a good tool for our investigation.

The rest of this paper is organized as follows: In Section II we present our model. First we describe our random walk model on a one-dimensional lattice with aperiodic disorder. Next we introduce the aperiodic sequences mentioned above and refer to their properties necessary for our study. In Section III multifractal analysis is performed. We describe the finite-size scaling formulation and discuss the criterion for classifying the localization property of the distribution and the finite-size effect. After briefly discussing the relationship with the inverse partitioning ratio, which characterizes the localization property, we present our results and discussion. Section IV is dedicated to the summary and future outlook.

II. MODEL

A. Random walk on a one-dimensional disordered lattice

Consider a one-dimensional random walk with only nearest neighbor hopping allowed. The time evolution of the probability for the particle to be on site j at time t, $p_j(t)$, is described by the master equation:

$$\frac{\partial p_j(t)}{\partial t} = w_{j-1,j}p_{j-1}(t) + w_{j+1,j}p_{j+1}(t) - (w_{j,j-1} + w_{j,j+1})p_j(t), \tag{7}$$

where $w_{j,k}$ denotes the transition rate for the particle to hop from site j to site k. Two transition rates are assigned to the j-th bond, which connects the j-th site to the $(j+1)$-th site. One is the forward rate $w_{j,j+1}$, and the other is the backward rate $w_{j+1,j}$. These transition rates are generally not symmetric, *i.e.*, $w_{j,j+1} \neq w_{j+1,j}$. Interestingly, in ref.[2], it is pointed out that the master equation Eq.(7) is equivalent to the transverse-field Ising model.

Let us take a binary sequence S, for example, $S = ABAABAABAB\cdots$. For this

sequence, the transition rates are assigned as

$$\frac{w_{j+1,j}}{w_{j,j+1}} = \begin{cases} a, & \text{the } j\text{-th bond is type } A, \\ b, & \text{the } j\text{-th bond is type } B. \end{cases} \tag{8}$$

If $a = b$, the one-dimensional lattice is homogeneous. It is apparent that the properties of the sequence S strongly affect the behavior of the random walk.

By definition, an aperiodic sequence has infinite length. We consider an aperiodic sequence which is constructed systematically by substitution rules and replace the fully aperiodic sequence with a finite approximant S_n of finite length L, where n denotes the generation of the approximant. We impose the periodic boundary conditions, $p_{j+L} \equiv p_j$, $w_{j+L,j+L+1} = w_{j,j+1}$, and $w_{j+L,j+L-1} = w_{j,j-1}$. The aperiodic sequence is recovered in the limit as $L \to \infty$.

We now consider the stationary probability distribution, $dp_j/dt = 0$. For simplicity, we set $w_{j,j+1} = 1$ for all j. The exact expression of the stationary probability is obtained[4] from the proportional relation

$$p_j \propto 1 + \sum_{k=1}^{L-1} \prod_{l=1}^{k} w_{j+l+1,j+l}, \tag{9}$$

and the normalization condition

$$\sum_{j=1}^{L} p_j = 1. \tag{10}$$

From this stationary probability, we can obtain the drift velocity (and the diffusion constant if Eq.(2) holds)[2, 4]. The drift velocity v_d is given as

$$v_d \propto 1 - \prod_{j=1}^{L} w_{j+1,j}, \tag{11}$$

If v_d is sufficiently large, the stationary probability distribution is extended throughout the system independently of the properties of the disorder. On the other hand, if v_d is small, diffusion is dominant and then the disorder of the lattice strongly affects the behavior of the system. Since we are interested in how the structure of the probability distribution is related to the diffusional behavior, we will consider only the case with vanishing drift velocity, *i.e.*, from Eq.(11),

$$\prod_{j=1}^{L} w_{j+1,j} = 1. \tag{12}$$

For a given a, b is given as a function of a so that Eq.(12) hold.

B. Aperiodic sequences

In this subsection, we review three aperiodic sequences, each of which we consider below for the disorder of a lattice. Following refs.[8, 9], we discuss the initial sequences, the substitution rules, which generate the sequences, and the wandering exponents. Then we will show the stationary probability distributions of our stochastic model with each of these types of aperiodic disorder.

1. Thue-Morse (TM) sequence

The TM sequence $S = ABBABAAB\cdots$ is generated by the initial sequence $S_1 = AB$ and the iterative substitution rules $A \to AB$ and $B \to BA$. Let $\#_n(A)$ and $\#_n(B)$ be the numbers of A and B, respectively, in the sequence of the n-th generation S_n. From the substitution rules, $\#_{n+1}(A)$ and $\#_{n+1}(B)$ are obtained from $\#_n(A)$ and $\#_n(B)$ as

$$\begin{bmatrix} \#_{n+1}(A) \\ \#_{n+1}(B) \end{bmatrix} = M \begin{bmatrix} \#_n(A) \\ \#_n(B) \end{bmatrix}, \tag{13}$$

where the substitution matrix M is given as

$$M = \begin{bmatrix} 1 & 1 \\ 1 & 1 \end{bmatrix}. \tag{14}$$

By diagonalizing the substitution matrix M, we find that the eigenvalues are $\lambda_1 = 2$ and $\lambda_2 = 0$, and

$$\#_{n+1}(A) + \#_{n+1}(B) = 2\{\#_n(A) + \#_n(B)\}, \tag{15}$$

$$\#_{n+1}(A) - \#_{n+1}(B) = 0. \tag{16}$$

From Eqs.(15) and (16) we obtain

$$\#_n(A) = \#_n(B) = 2^{n-1}. \tag{17}$$

For the n-th generation sequence S_n the length $L = \#_n(A) + \#_n(B)$ and the geometrical fluctuation $\Delta = \#_n(A) - \#_n(B)$ are $L = 2^n$ and $\Delta = 0$, respectively. From the definition of the wandering exponent $\Omega_{\rm TM}$, $\Delta \sim L^{\Omega_{\rm TM}}$, it is obtained as the ratio of the logarithm of (the absolute value of) the second-largest eigenvalue to the logarithm of the largest eigenvalue,

$$\Omega_{\rm TM} = \frac{\log|\lambda_2|}{\log\lambda_1} = -\infty. \tag{18}$$

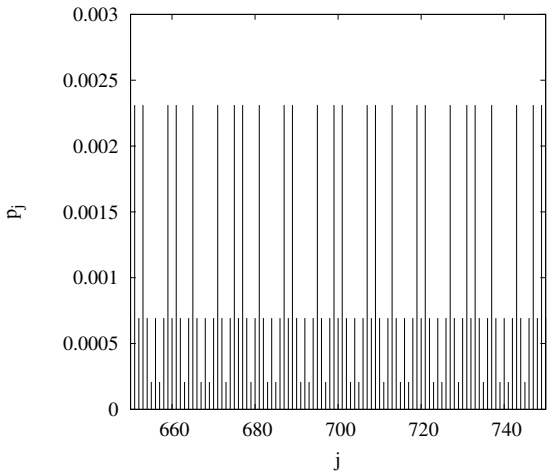

FIG. 1. Stationary probability distribution $\{p_j\}$ for the Thue-Morse model with $L = 1024$ and $a = 0.3$. For visibility, only the results of $650 \leq j \leq 750$ are shown. The distribution is extended.

Since $\#_n(A) = \#_n(B)$ holds in any generation, the vanishing drift velocity condition is $b = a^{-1}$.

Figure 1 shows the stationary probability distribution of the TM model with $L = 1024$ and $a = 0.3$. The diffusion of the TM model is known to be normal[2]. We observe that the distribution is extended. From Eq.(9), the distribution is analytically obtained in a simple form: For the n-th sequence S_n with a given a, the stationary probability distribution is composed of 2^{n-1} sites with $p_j = 1/C$, 2^{n-2} sites with $p_j = a/C$ and 2^{n-2} sites with $p_j = 1/aC$, where $C = 2^{n-1} + (a + a^{-1})2^{n-2}$ is the normalization constant. These three types of measures are aligned aperiodically.

2. Rudin-Shapiro (RS) sequence

The RS sequence $S = AAABAABA\cdots$ is generated by the initial sequence $S_1 = AA$ and the substitution rules $AA \to AAAB$, $AB \to AABA$, $BA \to BBAB$, and $BB \to BBBA$. In order to calculate $\#_n(A)$ and $\#_n(B)$ for the n-th sequence S_n, it is convenient to consider

$\#_n(AA)$, $\#_n(AB)$, $\#_n(BA)$, and $\#_n(BB)$. Using them, we obtain

$$\begin{bmatrix} \#_{n+1}(AA) \\ \#_{n+1}(AB) \\ \#_{n+1}(BA) \\ \#_{n+1}(BB) \end{bmatrix} = M \begin{bmatrix} \#_n(AA) \\ \#_n(AB) \\ \#_n(BA) \\ \#_n(BB) \end{bmatrix}, \tag{19}$$

where the 4×4 substitution matrix is

$$M = \begin{bmatrix} 1 & 1 & 0 & 0 \\ 1 & 0 & 1 & 0 \\ 0 & 1 & 0 & 1 \\ 0 & 0 & 1 & 1 \end{bmatrix}. \tag{20}$$

By diagonalizing the substitution matrix M, we find that the eigenvalues are 2, $\pm\sqrt{2}$, and 0, and for the first three eigenvalues,

$$\begin{aligned} &\#_{n+1}(AA) + \#_{n+1}(AB) + \#_{n+1}(BA) + \#_{n+1}(BB) \\ &= 2\{\#_n(AA) + \#_n(AB) + \#_n(BA) + \#_n(BB)\}, \end{aligned} \tag{21}$$

$$\begin{aligned} &(\sqrt{2}+1)\#_{n+1}(AA) + \#_{n+1}(AB) - \#_{n+1}(BA) - (\sqrt{2}+1)\#_{n+1}(BB) \\ &= \sqrt{2}\{(\sqrt{2}+1)\#_n(AA) + \#_n(AB) - \#_n(BA) - (\sqrt{2}+1)\#_n(BB)\}, \end{aligned} \tag{22}$$

$$\begin{aligned} &(\sqrt{2}-1)\#_{n+1}(AA) - \#_{n+1}(AB) + \#_{n+1}(BA) - (\sqrt{2}-1)\#_{n+1}(BB) \\ &= -\sqrt{2}\{(\sqrt{2}-1)\#_n(AA) - \#_n(AB) + \#_n(BA) - (\sqrt{2}-1)\#_n(BB)\}. \end{aligned} \tag{23}$$

From Eqs.(21)-(23),

$$\#_{n+1}(A) + \#_{n+1}(B) = 2\{\#_n(A) + \#_n(B)\}, \tag{24}$$

$$\#_{n+1}(A) - \#_{n+1}(B) = 2^{\lceil n/2 \rceil}\{\#_n(A) - \#_n(B)\}, \tag{25}$$

where $\lceil n/2 \rceil$ is the ceiling function:

$$\lceil n/2 \rceil = \begin{cases} n/2, & n \text{ even} \\ (n+1)/2. & n \text{ odd} \end{cases} \tag{26}$$

Then we immediately find that

$$\begin{aligned} \#_n(A) &= 2^{n-1} + 2^{\lceil n/2 \rceil - 1}, \\ \#_n(B) &= 2^{n-1} - 2^{\lceil n/2 \rceil - 1}, \end{aligned} \tag{27}$$

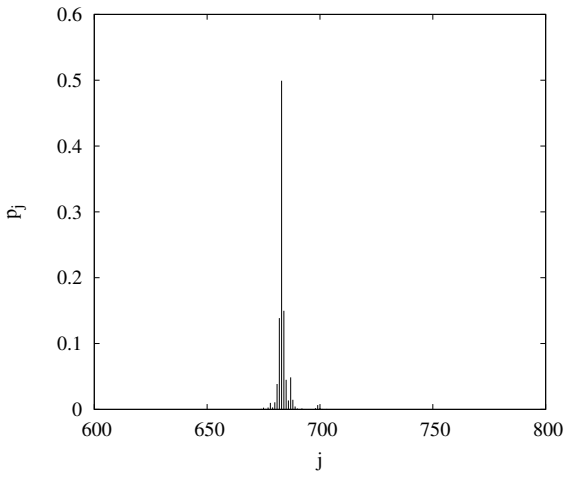

FIG. 2. Stationary probability distribution for the Rudin-Shapiro model with $L = 1024$ and $a = 0.3$. For visibility, Only the results of $600 \leq j \leq 800$ are shown. Clearly the distribution is localized.

and the length and geometrical fluctuation of the n-th sequence are $L = 2^n$ and $\Delta = 2^{\lceil n/2 \rceil}$, respectively. This last result means that the geometrical fluctuation scales as $\Delta \sim 2^{n/2}$, which corresponds to the second-largest eigenvalues, $\pm\sqrt{2}$.

The wandering exponent $\Omega_{\rm RS}$ is

$$\Omega_{\rm RS} = \frac{\log\sqrt{2}}{\log 2} = \frac{1}{2}. \tag{28}$$

The geometrical fluctuation of the RS sequence grows unboundedly with the sequence length as $\Delta \sim L^{1/2}$. Note that the value $\Omega_{\rm RS} = 1/2$ coincides with that of the random binary sequence.

For the drift velocity to vanish, $b = a^{-\#_n(A)/\#_n(B)}$ for a given a. In the limit as $n \to \infty$, b approaches a^{-1}. The stationary probability distribution of the RS model with $a = 0.3$ and $L = 1024$ is shown in FIG.2. The distribution is strongly localized. It was reported that diffusion is ultlaslow in the RS model, where the mean square displacement scales as Eq.(3)[2].

3. Paperfolding (PF) sequence

The PF sequence $S = AABAABBA\cdots$ is generated by the initial sequence $S_1 = AA$ and the substitution rules $AA \to AABA$, $AB \to AABB$, $BA \to ABBA$, and $BB \to ABBB$.

The recursion relation for the numbers of letters A and B is expressed in the same form as Eq.(19), where the substitution matrix in this case is given as

$$M = \begin{bmatrix} 1 & 1 & 0 & 0 \\ 0 & 0 & 1 & 1 \\ 1 & 0 & 1 & 0 \\ 0 & 1 & 0 & 1 \end{bmatrix}. \tag{29}$$

The eigenvalues of M are 2, 1, and 0 (which is doubly degenerate), and for the first two eigenvalues,

$$\begin{aligned} &\#_{n+1}(AA) + \#_{n+1}(AB) + \#_{n+1}(BA) + \#_{n+1}(BB) \\ &= 2\{\#_n(AA) + \#_n(AB) + \#_n(BA) + \#_n(BB)\}, \end{aligned} \tag{30}$$

$$\begin{aligned} &\#_{n+1}(AA) - \#_{n+1}(AB) + \#_{n+1}(BA) - \#_{n+1}(BB) \\ &= \#_n(AA) - \#_n(AB) + \#_n(BA) - \#_n(BB), \end{aligned} \tag{31}$$

We find that for the n-th sequence $L = 2^n$, $\Delta = 2$, and

$$\begin{aligned} \#_n(A) &= 2^{n-1} + 1, \\ \#_n(B) &= 2^{n-1} - 1. \end{aligned} \tag{32}$$

The wanderling exponent of the PF sequence vanishies:

$$\Omega_{\mathrm{PF}} = \frac{\log 1}{\log 2} = 0. \tag{33}$$

In fact the geometrical fluctuation grows logarithmically with L although it remains constant at the endpoint.

For the drift velocity to vanish,

$$b = a^{-(2^{n-1}+1)/(2^{n-1}-1)}, \tag{34}$$

for a given a, which converges to a^{-1} in the limit as $n \to \infty$. It was found that in the PF model, the diffusion is anomalous, and it is written as in Eq.(4)[2], where the exponent ϕ depends on the inhomogeneity parameter a. The stationary probability distribution of the PF model with $a = 0.3$ and $L = 1024$ is shown in FIG.3. The distribution appears to be singular, and appears to be neither extended nor localized. We can observe its complex and hierarchical structure.

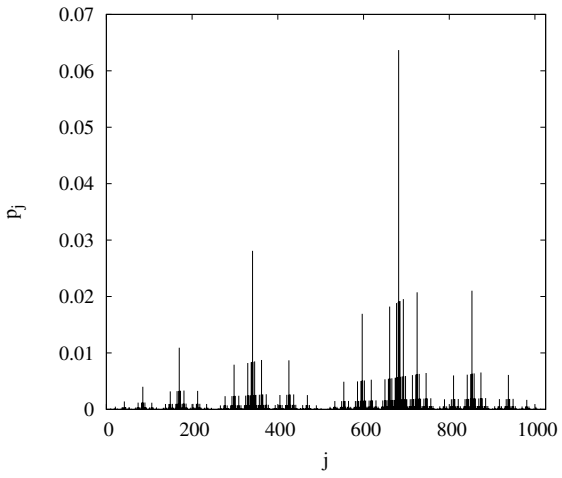

FIG. 3. Stationary probability distribution for the paperfolding model with $L = 1024$ and $a = 0.3$. A complex and hierarchical structure ca be observed.

III. MULTIFRACTAL ANALYSIS

A. Formulation: on a one-dimensional support

Aperiodic chains are defined in the limit as $L \to \infty$. Thus we estimate the results of the system as $L \to \infty$ by systematically extrapolating from the results of systems with finite L.

Let us review the formulation of multifractal on a one-dimensional support[10, 11]. Suppose that a stationary probability measure for a finite one-dimensional L-site system $\{p_j\}_{j=1,2,\cdots,L}$ is given. The partition function $Z(q, L)$ is introduced as

$$Z(q, L) = \sum_{j, p_j \neq 0} (p_j)^q. \tag{35}$$

The multifractal exponent for the finite system $\tau(q, L)$ is defined as

$$\tau(q, L) = -\frac{\log Z(q, L)}{\log L}. \tag{36}$$

By the Legendre transformation, the singularity exponent α for the finite system and its fractal dimension $f(\alpha)$ are obtained, as functions of q and L:

$$\alpha(q, L) = \frac{\partial \tau(q, L)}{\partial q}, \tag{37}$$

$$f(\alpha(q, L)) = q\alpha(q, L) - \tau(q, L). \tag{38}$$

However it is not practical to evaluate α and $f(\alpha)$ numerically from Eqs.(37) and (38), since this requires numerical differentiation, which may produce relatively large errors. Therefore it is better to evaluate them directly. We show this below, following the method presented in ref.[12].

Let us construct a new probability measure $\{\mu_j(q)\}$ from $\{p_j\}$:

$$\mu_j(q) = \frac{(p_j)^q}{\sum_{j=1}^{L}(p_j)^q}. \tag{39}$$

Then let us define $\zeta(q, L)$ and $\xi(q, L)$ as

$$\zeta(q, L) = \sum_{j=1}^{L} \mu_j(q) \log p_j, \tag{40}$$

$$\xi(q, L) = \sum_{j=1}^{L} \mu_j(q) \log \mu_j(q), \tag{41}$$

from which we obtain $\alpha(q, L)$ and $f(\alpha(q, L))$ as

$$\alpha(q, L) = -\frac{\zeta(q, L)}{\log L}, \tag{42}$$

$$f(\alpha(q, L)) = -\frac{\xi(q, L)}{\log L}. \tag{43}$$

Direct calculation shows that the definitions Eqs.(42) and (43) satisfy the relations Eqs.(37) and (38). Note that the above formulation has some similarities with the thermodynamic formulation of the Rényi entropy $H(q)$ of dynamical systems, which is defined as[15]

$$H(q) = \frac{1}{1-q} \log \left[\sum_j (p_j)^q \right], \tag{44}$$

for $q > 0$. The phase transition related to the Rényi entropy of a deterministic chaotic system is discussed in ref.[6].

Next we estimate the finite size effect. For example, the "true" value of $\tau(q)$ for a system of infinite size is defined as

$$\tau(q) = \lim_{L \to \infty} \tau(q, L), \tag{45}$$

and $\alpha(q)$ and $f(\alpha(q))$ are defined similarly. They should be obtained by careful extrapolation from the results for systems of finite size. From Eqs.(35), (36) and (45), we expect that

$$\tau(q) - \tau(q, L) = \mathcal{O}(1/\log L). \tag{46}$$

Therefore we estimate the value of $\tau(q)$ from the plot of $\tau(q, L)$ against $1/\log L$ and the extrapolation to $1/\log L \to 0$.

The localization property of a given distribution can be read from its multifractal spectrum, especially the results for $q \to \pm\infty$. This is known in quantum localization problem, where the probability distribution is given as the squared norm of the wavefunction[11]. Let $\alpha_{\min}$ and $\alpha_{\max}$ be $\alpha(q \to \infty)$ and $\alpha(q \to -\infty)$, respectively, and let $f_{\min} = f(\alpha_{\min})$ and $f_{\max} = f(\alpha_{\max})$. For an extended distribution, the multifractal spectrum of the systems of finite size converges to a single point $\alpha = f = 1$ in the limit as $L \to \infty$. For a localized distribution, $\alpha_{\min}$ and $f_{\min}$ converge to 0, $\alpha_{\max}$ diverges to infinity, and $f_{\max}$ converges to unity. For a singular distribution, $\alpha_{\min}$ and $\alpha_{\max}$ take different finite values. The spectrum $f(\alpha)$ is a continuous and convex curve which takes values only within $\alpha \in [\alpha_{\min}, \alpha_{\max}]$.

B. Localization and inverse participation ratio

Note that the partition function Eq.(35) with $q = 2$, $Z(q = 2, L)$ is equivalent to the "inverse participation ratio (IPR)" . The IPR was originally introduced in quantum localization problem[16, 17] more than forty years ago. Its purpose is to simply evaluate the localization property of a given distribution. It has been used not only in quantum mechanics but also even in finance[18]. And some generalizations have been attempted recently[19, 20]. The scaling behavior of the IPR against the system size L is used to classify the localization property of a given distribution. If a state is extended, the IPR is inversely proportional to the system size, since the probability measure at a site is roughly inversely proportional to the system size, *i.e.*, $p_j \sim L^{-1}$. On the other hand, if a state is localized, the IPR is almost independent of the system size. If a state is singular, which is called "critical" in the context of quantum localization, the scaling behavior of the IPR is intermediate between the behavior in the above two cases:

$$IPR(L) \sim L^{-\delta} \quad \text{with } 0 < \delta < 1. \tag{47}$$

We expect that these scaling behaviors hold for the stationary probability distribution of our classical stochastic models.

Figure 4 shows the log-log plots of the IPR against the system size L for the TM, RS, and PF models with $a = 0.3$. For the TM model, it is observed that $Z(2, L) \sim L^{-1}$.

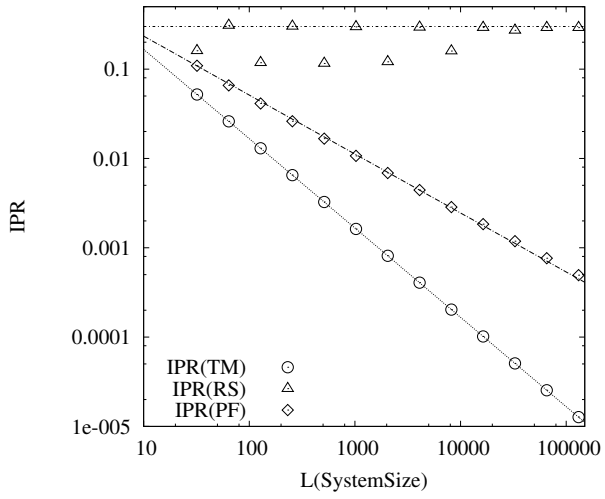

FIG. 4. Log-log plots of the inverse participation ratio $Z(2, L)$ against system size L for the Thue-Morse, Rudin-Shapiro, and paperfolding models with $a = 0.3$. Lines are, from top to bottom, $Const.$, $L^{-0.69}$, and L^{-1}.

For the RS model, for small n, the IPR depends on whether $n = \log_2 L$ is even or odd. However, as n increases, the series of the results for odd n converge with those for even n, and the results become independent of the system size, *i.e.*, $Z(2, L) \sim Const.$ These results are consistent with the localization properties of their probability distributions as shown in FIGs.1 and 2, which are extended for the TM model and localized for the RS model, respectively. These scaling properties are independent of the value of a. For the PF model with a singular probability distribution, the scaling behavior is $Z(2, L) \sim L^{-\delta}$ with $\delta = 0.69$. Note that in this case, the exponent δ depends on a. Figure 5 shows the a-dependence of δ. It monotonically increases with a and approaches 1 as $a \to 1$, since the system with $a = 1$ is homogeneous and so the distribution is extended.

C. Multifractal Spectra

Since $\alpha_{\max}$ and $f_{\max}$ are dominated by the smallest measure of the distribution, they may have large numerical errors. Therefore we will restrict our discussion to only $\alpha_{\min}$ and $f_{\min}$.

Figure 6 shows the plots of $\alpha_{\min}(L)$ against $1/n = 1/\log_2 L$ for the TM, RS, and PF models with $a = 0.3$. For the TM and PF models, these plots are linear. For the RS

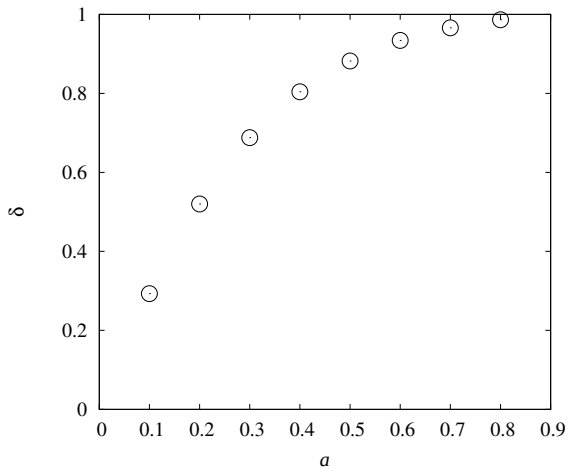

FIG. 5. Plots of the exponent δ in Eq.(47) against a. In the homogeneous limit $a \to 1$, $\delta \to 1$.

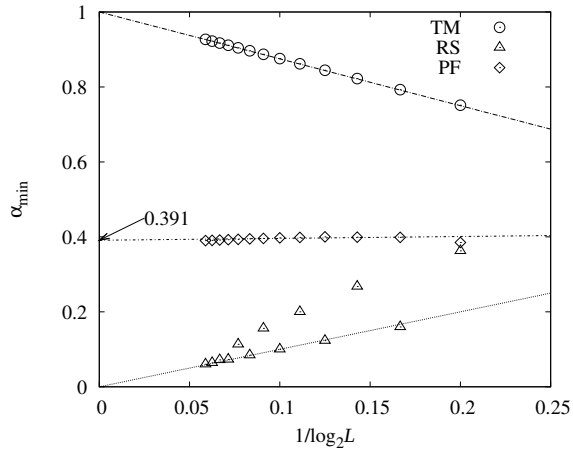

FIG. 6. Plots of $\alpha_{\min}(L)$ against $1/n = 1/\log_2 L$ for the Thue-Morse, Rudin-Shapiro, and paperfolding model with $a = 0.3$. Their linear dependence means that the leading correction is $\mathcal{O}(1/\log L)$.

model, similar to the case of the scaling of the IPR, some parity dependence is found for small n. However, for large n the plots become linear, independent of the parity of n. This validates our expectation of the finite-size effect, Eq.(46). Extrapolating the plots toward $1/\log L \to 0$, we find that $\alpha_{\min} \to 1$ for the TM model, $\alpha_{\min} \to 0$ for the RS model, and $\alpha_{\min} \to \sim 0.391$ for the PF model. Figure 7 shows the plots of $f_{\min}(L)$ against $1/\log_2 L$. It can be observed that in the limit as $1/\log L \to 0$, $f_{\min} \to 1$ for the TM model, and $f_{\min} \to 0$

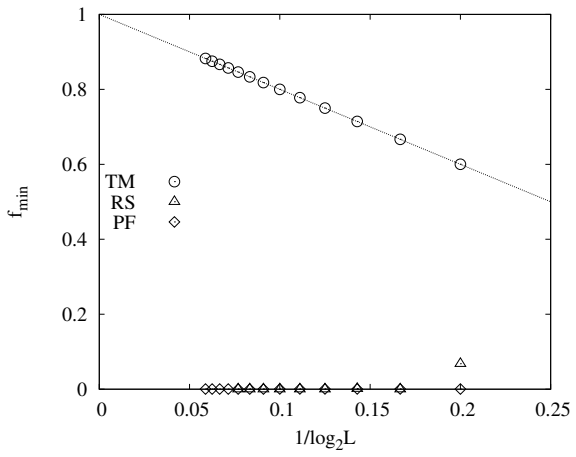

FIG. 7. Plots of $f_{\min}(L) = f(\alpha_{\min}(L))$ against $1/\log_2 L$ for the Thue-Morse, Rudin-Shapiro, and paperfolding model with $a = 0.3$. The leading correction here is also $\mathcal{O}(1/\log L)$.

for the RS and PF models. These results are consistent with the criteria mentioned in the last paragraph of Sec.III A and also with the results of the IPR scaling behavior obtained in Sec.III B.

For the PF model, the multifractal $f(\alpha)$ spectrum takes continuous values within $\alpha \in [\alpha_{\min}, \alpha_{\max}]$, where $\alpha_{\min}$ and $\alpha_{\max}$ are both positive finite values. The multifractal spectrum for the PF model with $a = 0.3$ is shown in FIG.8. It is convex upwards, which is a universal property, and takes the maximum value $f = 1$, reflecting the fact that the support of the probability distribution is one-dimensional. Moreover it looks symmetric with respect to $\alpha = \alpha_0$, where it takes the maximum. This result is in quite good agreement with the spectrum of the "binomial branching process", which is a simple process constructed by the recursion of elementary uneven partitioning. The binomial partitioning process was first introduced as a simple model for the hierarchical energy cascade of turbulence[21]. It has been applied as a simple model for various systems including the sidebranch structure of a dendrite[14] and fragmentation[22]. In this process, the spectrum can be calculated exactly due to its simplicity:

$$\alpha(q) = -\frac{\eta \log p + (1-\eta)\log(1-p)}{\log 2}, \tag{48}$$

$$f(\alpha(q)) = -\frac{\eta \log \eta + (1-\eta)\log(1-\eta)}{\log 2}, \tag{49}$$

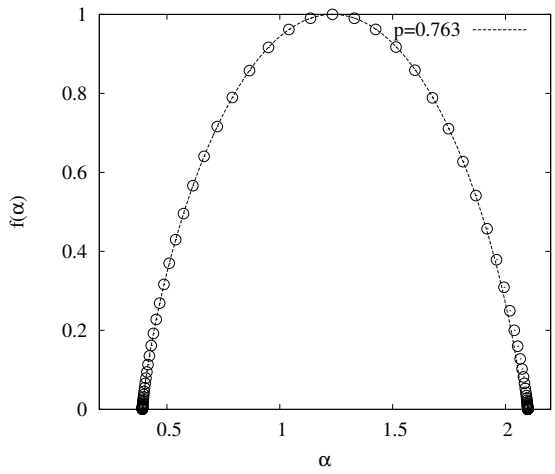

FIG. 8. Multifractal $f(\alpha)$ spectrum of the stationary probability distribution of the PF model with $a = 0.3$ and that of the binomial branching process with $p = 0.763$.

where

$$\eta = \frac{p^q}{p^q + (1-p)^q}, \tag{50}$$

and $1/2 < p < 1$ is the partitioning parameter, which is the only free parameter in the process. From Eq.(48) we immediately obtain $\alpha_{\min} = -\log_2 p$ and $\alpha_{\max} = -\log_2(1-p)$. This agreement shows that, in the PF model, there exists a mechanism which partitions the probability measure unevenly and hierarchically, in a way similar to that in the binary branching process. This is attributed to the fact that the effect of the fluctuation of the PF sequence, due to its vanishing wandering exponent, is almost independent of length scale.

Figure 9 shows the a-dependence of $\alpha_{\min}$. We find that $\alpha_{\min}$ is a monotonically increasing function of a. In the limit as $a \to 1$, the system becomes homogeneous, and therefore the distribution is extended and $\alpha_{\min}$ approaches unity, which characterizes an extended distribution. Since the multifractal spectra for the PF model and the binary partitioning process are in good agreement, the parameter in the binary branching process, p, and a are related as $\alpha_{\min}(a) = -\log_2 p$.

Thus far, we have restricted ourselves to the case of $a < 1$ for each model. For $a > 1$, at least the localization property of the probability distribution and the multifractal spectra do not vary under $a \leftrightarrow a^{-1}$, in the limit as $L \to \infty$. This is probably a consequence of the fact that in the underlying aperiodic sequence, the ratio of the number of A to that of B converges to unity.

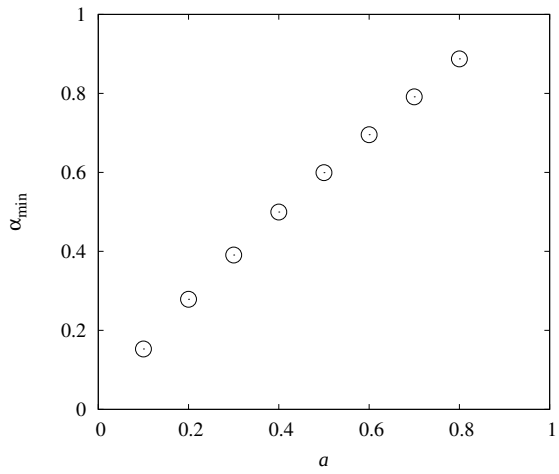

FIG. 9. Plot of $\alpha_{\min}$ against a. The value of $\alpha_{\min}$ converges to unity in the homogeneous limit as $a \to 1$.

IV. SUMMARY AND OUTLOOK

We found that the stationary probability distribution of a random walk on a one-dimensional aperiodically disordered lattice shows a characteristic localization pattern which corresponds to its diffusional behavior. The results are summarized in TABLE I. The localization pattern of the distribution (extended, localized, or singular) depends on the wandering exponent of the background aperiodic sequence. These types of pattern can be distinguished by the finite-size scaling of the partition function $Z(q = 2, L)$, the singular exponent $\alpha_{\min}$, and the fractal dimension $f_{\min}$. In particular, for the distribution of the model with a vanishing wandering exponent, we obtained a continuous multifractal spectrum with finite $\alpha_{\min}$ and $\alpha_{\max}$ ($\alpha_{\min} \neq \alpha_{\max}$). This spectrum reflects the singular and hierarchical structure of the distribution and agrees well with the spectrum of the binomial branching process.

We considered only the case with a vanishing drift velocity $v_d = 0$, since we were interested in the diffusional behavior. As mentioned in Section II A, a finite drift velocity $v_d \neq 0$ causes a finite current through the lattice and makes the distribution extended. It may be an interesting problem to determine how a localized or singular distribution changes by a finite drift velocity.

Sequence	Ω	PDF	Diffusion	$\alpha_{\min}$	$f_{\min}$
TM	-	extended	normal	1	1
RS	+	localized	ultraslow	0	0
PF	0	singular	anomalous	finite	0

TABLE I. Summary of the results. Ω denotes the wanderling exponent, PDF denotes the stationary probability distribution function, and $\alpha_{\min}$ and $f_{\min}$ denote $\alpha(q \to \infty, L \to \infty)$ and $f(q \to \infty, L \to \infty)$, respectively.

ACKNOWLEDGMENTS

The author would like to thank Professor H.Honjo for useful comments.

Appendix: Binomial branching process

We discuss the binomial branching process[21] so that this article is self-contained. Its multifractal spectrum can be exactly calculated due to its simple structure.

Suppose that a segment of length 1 is divided into two segments of length 1/2. A probability measure $p > 1/2$ is assigned to the left segment and $(1-p)$ to the right. This p is the only free parameter of the process. Next, each segment is subdivided into two equal halves and the measure is partitioned into p to the left and $(1-p)$ to the right. There are now four segments, each of length 1/4, and the measures p^2, $p(1-p)$, $(1-p)p$, and $(1-p)^2$ are assigned to the segments from left to right. This procedure is iterated (see FIG.10), which shows the hierarchical structure $n = 8$. At the n-th stage, there are 2^n segments, each of length 2^{-n} and the number of segments with measure $p^k(1-p)^{n-k}$, $k = 0, 1, \cdots, n$, is $\binom{n}{k} = n!/[k!(n-k)!]$. Therefore the partition function for this stage, $Z(q,n)$ is immediately obtained as

$$\begin{aligned} Z(q,n) &= \sum_{k=0}^{n} \binom{n}{k} [p^k(1-p)^{n-k}]^q \\ &= [p^q + (1-p)^q]^n. \end{aligned} \tag{A.1}$$

The multifractal exponent $\tau(q)$ is, in the limit as $n \to \infty$:

$$\tau(q) = -\frac{\log[p^q + (1-p)^q]}{\log 2}. \tag{A.2}$$

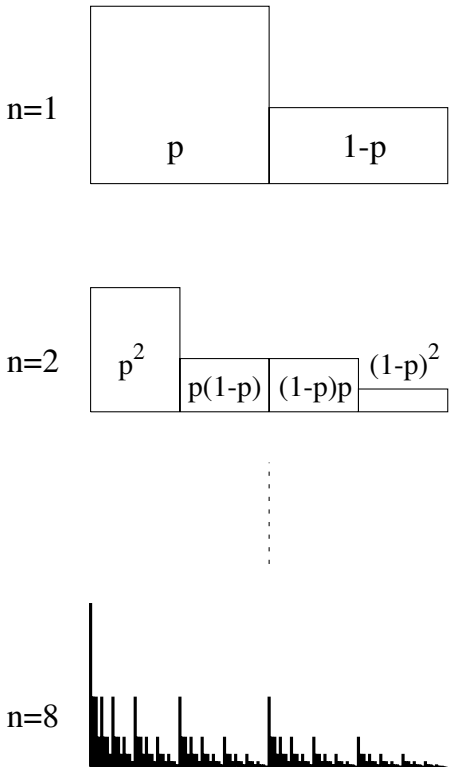

FIG. 10. Different stages of the binomial branching process. Each segment is divided into two equal subsegments at the next stage and its measure is divided into nonequal fractions, p and $(1-p)$. This figure is cited from ref.[14].

From this and by using the Legendre transformation the singularity exponent $\alpha(q)$ and the fractal dimension $f(\alpha(q))$ are obtained as Eqs.(48) and (49). The direct evaluation, Eqs.(42) and (43), gives the same result. The spectrum is symmetric with respect to $\alpha_0 = -[\log_2 p + \log_2(1-p)]/2$ and takes the maximum $f(\alpha_0) = 1$, which reflect the fact that the support is one-dimensional.

---

[1] J.-P.Bouchaud and A.Georges, Phys.Rep. **195**, 127(1990).

[2] F.Iglói, L.Turban and H.Rieger, Phys.Rev.E **59**, 1465(1999).

[3] Y.G.Sinai, Theor.Probab.Appl. **27**, 247(1982).

[4] B.Derrida, J.Stat.Phys. **31**, 433(1983).

[5] J.Dräger and J.Klafter, Phys.Rev.Lett. **84**, 5998(2000).

[6] R.Venegeroles, Phys.Rev.E **86**, 021114(2012). J.Stat.Phys.**154**, 988(2014);

[7] L.Dal Negro, J.H.Yi.V.Nguyen, Y.Yi.J.Michel and L.C.Kimerling, Appl.Phys.Lett.**86**, 261905(2005); V.Passias, N.V.Valappil, Z.Shi, L.Deych, A.A.Lisyansky and V.M.Menon, Opt.Exp. **17**, 6636(2009).

[8] J.M.Luck, J.Stat.Phys. **72**, 417(1993).

[9] J.Hermisson, J.Phys.A **33**, 57(2000).

[10] T.C.Halsey, M.H.Jensen, L.P.Kadanoff, I.Procaccia, and B.I.Shraiman, Phys.Rev.A **33**, 1141(1986).

[11] H.Hiramoto and M.Kohmoto, Int.J.Mod.Phys.B **6**, 281(1992), *and references therein.*

[12] A.Chhabra and R.V.Jensen, Phys.Rev.Lett. **62**, 1327(1989).

[13] A.B.Chhabra, C.Meneveau, R.V.Jensen and K.R.Sreenivasan, Phys.Rev.A **40**, 5284(1989).

[14] H.Miki and H.Honjo, J.Phys.Soc.Jpn. **82**, 034002(2013).

[15] J.-P.Eckmann and D.Ruelle, Rev.Mod.Phys. **57**,617(1985); C.Tsallis, J.Stat.Phys. **52**, 479(1988).

[16] R.J.Bell and P.Dean, Discuss. Faraday Soc. **50**, 55(1970).

[17] D.J.Thouless, Phys.Rep. **13C**, 63(1974).

[18] V.Plerou, P.Gopikrishnan, B.Rosenow, L.A.Nunes Amaral and H.E.Stanley, Phys.Rev.Lett. **83**, 1471(1999).

[19] N.C.Murphy, R.Wortis and W.A.Atkinson, Phys.Rev.B **83**, 184206(2011).

[20] L.Yang, N.Yang and B.Li, Sci.Rep. **3**, 1143(2013).

[21] C.Meneveau and K.R.Sreenivasan, Phys.Rev.Lett. **59**, 1424(1987).

[22] H.Katsuragi, D.Sugino and H.Honjo, Phys.Rev.E **68**, 046105(2003); Phys.Rev.E **70**, 065103(R)(2004).